2014 IEEE International Conference on Computer and Information Technology

Study of Multistatic Radar against False Targets Jamming using Spatial Scattering Properties

Shanshan Zhao, Linrang Zhang, Yu Zhou, Nan Liu
National Laboratory of Radar Signal Processing
Xidian University
Xi'an, China
zhaoshanshan025@163.com, lrzhang@xidian.edu.cn, zhouyu@mail.xidian.edu.cn, liunaneoe@163.com

Abstract—**This paper presents a discrimination method of deception false targets in multistatic radar system using signal fusion. Based on the difference in spatial scattering properties between physical targets and false targets, correlation test is used on the complex envelope sequences to identify false targets, which is formulated as a problem of likelihood ratio test in the Neyman-Pearson sense. The simulation results verify the efficiency of the approach to discriminate false targets on the premise of the acceptance probability of physical targets.**

Keywords—false targets; multistatic radar; signal fusion; spatial scattering property; likelihood ratio test

I. INTRODUCTION

Deception jamming has become a crucial self-screening jamming against tracking radar because of its high effectivity. With the development of digital-radio-frequency memory (DRFM) technology, jammers are able to generate multiple false targets (FTs) surrounding desired radar echoes that are highly correlated with real radar echoes and probably overlap with the physical target (PT) signals in both time and frequency domain [1]. These "intelligent" FTs can easily confuse the radar processing circuitry and exhaust the radar resources.

In order to combat deception jamming, transmitting signal optimization [2], polarization characters [3], motion features [4] and DRFM quantization error [5] are used to differentiate FTs in monostatic radar. In [6, 7], two identification methods of deception false targets, respectively in bistatic radar and netted radar, are presented based on data correlation algorithm using the fact that a jammer can hardly generate false target signals to each station that seem to be originated from common target sources. Besides, Doppler frequencies to all stations are not equal for PTs, but equal for velocity deception jamming. Exploiting this difference, radar ECCM against velocity-deception jamming in multistatic radar is provided in [8, 9]. However, it must be pointed out that most anti-jamming methods available are implemented by data fusion, which cannot fully explore the anti-jamming abilities of multistatic radar considering that lots of information (e.g., amplitude, phase of target echoes) is indubitably discarded in the process of measuration. So it is of paramount importance for countering deception jamming by signal fusion which is defined as a direct fusion of target echoes.

This work was supported by the National Natural Science Foundation of China under Grant 61301285, 61301281.

Due to radar cross section (RCS) spatial variations, targets display essentially independent scattering returns when radiated from sufficiently different directions [10, 11]. In contrast, "echoes" of a FT are fully correlated despite of the differences in the signal strength caused by antenna gain and path loss effects, because all the "echoes" are caused by one deception jamming. With this difference in spatial scattering properties serving as the theoretical basis, an active FTs discrimination method by signal fusion is proposed in the paper. After being countered by our method, FTs can be then identified using existing approaches by data fusion to raise the discrimination ratio of FTs further.

The rest of the paper is organized as follows. Section II introduces the signal model for multistatic radar with deception jamming. Spatial scattering properties of PTs and FTs are analyzed in detail. In section III, a discrimination method based on correlation tests (CTs) is proposed and its performance analysis is given in theory. Section IV presents the simulation results. Conclusion is drawn in Section V.

II. SIGNAL MODEL

Consider multistatic radar consisting of a transmitter and N sufficiently spaced receivers, simultaneously detecting K PTs with a deception jammer. In order to protect these PTs, M active FTs are generated surrounding them, which might be generated by range, Doppler, or angle deception jamming.

The spatial scattering properties of PTs and FTs are reflected by the mutual correlation of target echo signals [11]. Therefore, considering a fast fluctuating target, a complex envelope sequence of a target in slow-time domain for several consecutive pulse repeat intervals (PRIs), called a slow-time complex envelope sequence (SCES), is introduced to describe the correlation. With probability of detection one, $K+M$ targets (PTs and FTs) will be detected in each receiver, and the p-th SCES in receiver n is given by

$$\boldsymbol{A}_p^n = \boldsymbol{B}_p^n + \boldsymbol{W}^n \tag{1}$$

where, p=1,2,…,$K+M$, $\boldsymbol{W}^n$ represents the noise sequence with a distribution as $\boldsymbol{W}^n \sim \mathcal{CN}\left(0, \sigma_{w,n}^2 \mathbf{I}_{Q\times Q}\right)$, $\mathbf{I}$ denotes the identity matrix, and Q is the number of PRIs used to compose a SCES. $\boldsymbol{B}_p^n$ represents the complex amplitude contributed by

978-1-4799-6239-6/14 $31.00 © 2014 IEEE
DOI 10.1109/CIT.2014.132

the target signal strength in the SCES, called a slow-time complex amplitude sequence (SCAS), which is just the SCES without noise, i.e.,

$$\boldsymbol{B}_p^n = \begin{cases} [\alpha_{p,n}^1, \alpha_{p,n}^2, ..., \alpha_{p,n}^q, ..., \alpha_{p,n}^Q]^T, & \text{the } p\text{-th target is a PT} \\ [\beta_{p,n}^1, \beta_{p,n}^2, ..., \beta_{p,n}^q, ..., \beta_{p,n}^Q]^T, & \text{the } p\text{-th target is a FT} \end{cases} \quad (2)$$

where, superscript q represents the order number of PRIs, q=1,2,…,Q. The superscript "T" denotes the transpose operator.

In the following subsection, Mutual correlations of SCESs in different receivers for PTs and FTs are analyzed, which are the basis and prerequisite for the discrimination approach.

A. Mutual Correlation of SCESs for PTs

Invoking the central limit theorem (CLT), the distribution of $\alpha_{p,n}^q$ is approximately as $\alpha_{p,n}^q \sim \mathcal{CN}\left(0, \sigma_{p,n}^2\right)$ with $\sigma_{p,n}^2$ as its variance. And the components of the SCAS in (2) for a PT, denoted by $\boldsymbol{B}_{p|\mathrm{PT}}^n$, are independent identical distributed (i.i.d.). Then the distributions of $\boldsymbol{B}_{p|\mathrm{PT}}^n$ and $\boldsymbol{A}_{p|\mathrm{PT}}^n$ are approximately as,

$$\boldsymbol{B}_{p|\mathrm{PT}}^n \sim \mathcal{CN}\left(\mathbf{0}, \sigma_{p,n}^2 \mathbf{I}_{Q\times Q}\right) \quad (3)$$

$$\boldsymbol{A}_{p|\mathrm{PT}}^n \sim \mathcal{CN}\left(\mathbf{0}, (\sigma_{p,n}^2 + \sigma_{w,n}^2)\mathbf{I}_{Q\times Q}\right) \quad (4)$$

As mentioned above, the complex amplitudes $\{\alpha_{p,n}^q\}_{n=1}^L$ of a same PT in different receivers are independent, as a result of which SCASs in different receivers for a same PT are mutually orthogonal, $E\left[(\boldsymbol{B}_{p|\mathrm{PT}}^n)^H \boldsymbol{B}_{p|\mathrm{PT}}^{n'}\right] = 0$. Moreover, because of the independence of noise in different receivers represented by $E[(\boldsymbol{W}^n)^H \boldsymbol{W}^{n'}] = 0$, SCESs are also mutually orthogonal, i.e.,

$$E\left[(\boldsymbol{A}_{p|\mathrm{PT}}^n)^H \boldsymbol{A}_{p|\mathrm{PT}}^{n'}\right] = 0 \quad (5)$$

where the superscript "H" denotes the Hermitian operator.

B. Mutual Correlation of SCESs for FTs

Generally, FTs with a stochastic fluctuation in complex amplitudes can obtain a better deception performance. Without loss of generality, the complex amplitudes of FTs here are modeled as a random variable with a normal distribution, i.e., $\beta_{p,n}^q \sim \mathcal{CN}\left(0, \tilde{\sigma}_{p,n}^2\right)$, similar to that of a PT.

Since FTs in different receivers are generated by the same deception jamming signals, SCASs in different receivers for the same FT (i.e., generated by one deception signal), denoted by $\boldsymbol{B}_{p|\mathrm{FT}}^n$, are fully correlated, i.e., $\boldsymbol{B}_{p|\mathrm{FT}}^n = k \cdot \boldsymbol{B}_{p|\mathrm{FT}}^{n'}$ for $n \neq n'$, where $|k| = \tilde{\sigma}_{p,n'} / \tilde{\sigma}_{p,n}$. With the existence of independent noise sequence $\boldsymbol{W}^n$, SCESs in different receivers, similarly written as $\boldsymbol{A}_{p|\mathrm{FT}}^n$, are no longer linear related, but still correlated. And the mutual correlation of $\boldsymbol{A}_{p|\mathrm{FT}}^n$ and $\boldsymbol{A}_{p|\mathrm{FT}}^{n'}$ is given by

$$E\left[(\boldsymbol{A}_{p|\mathrm{FT}}^n)^H \boldsymbol{A}_{p|\mathrm{FT}}^{n'}\right] = E\left[(\boldsymbol{B}_{p|\mathrm{FT}}^n)^H \boldsymbol{B}_{p|\mathrm{FT}}^{n'}\right] = Q \cdot \sqrt{\tilde{\sigma}_{p,n}^2 \tilde{\sigma}_{p,n'}^2} \quad (6)$$

which is in proportion to the number of PRIs Q and the jamming power.

III. Discrimination Method

Based on the difference of spatial scattering properties of PTs and FTs, correlation tests are proposed to identify FTs. Without loss of generality, the discrimination approach is given in the case of $N = 2$ for simplification.

A. Correlation Test

In order to measure the difference in mutual correlation of two SCESs in receiver 1 and 2, define the correlation metric (CM) as,

$$\mu_{pp'} = \mathrm{Re}\left((\boldsymbol{A}_p^1)^H \boldsymbol{A}_{p'}^2\right) \quad (7)$$

which is the real component of the estimation of mutual correlation to ensure the CM being real-valued.

It should be noted that the sources of targets in each receiver are unknown and that the corresponding relations among them are also uncertain before the discrimination. Therefore, a traverse for all the possible combinations $\left\{\boldsymbol{A}_p^1, \boldsymbol{A}_{p'}^2 \middle| \forall p, \forall p' = 1,2,...,K+M\right\}$ is inevitable, as a result of which more situations might happen except for the two given in Section II. Then the problem of CTs is formulated here as a multiple hypothesis testing (MHT) problem on the CM for all combinations computed by (7) with four hypotheses.

- Under the null hypothesis (H_0) it is assumed that the combination consists of two PTs (originate from the same target source or not).
- Under the first hypothesis (H_1) it is assumed that the combination consists of a PT and a FT.
- Under the second hypothesis (H_2) it is assumed that the combination consists of two FTs generated by two different deception signals.
- Under the third hypothesis (H_3) it is assumed that the combination consists of two FTs generated by one deception signal.

Under H_0, H_1 and H_2, $\boldsymbol{A}_p^1$ and $\boldsymbol{A}_{p'}^2$ are two independent identical distributed stochastic sequences with a complex normal distribution. Then, $\mu_{pp'}$ is a sum of $2Q$ i.i.d. random variables, which are the products of two independent real Gaussian random variables. According to the CLT, $\mu_{pp'}$ can be approximately normal with zero mean and variance

$$D[\mu_{pp'} | H_0] = \frac{Q}{2} \zeta_{p,1}^2 \zeta_{p',2}^2 \quad (8)$$

where $\zeta_{p,1}^2$ and $\zeta_{p',2}^2$ are the second moment or the average power of the components of $\boldsymbol{A}_p^1$ and $\boldsymbol{A}_{p'}^2$, respectively.

Under H_3, $\boldsymbol{A}_p^1$ and $\boldsymbol{A}_{p'}^2$ are generated by one deception signal, as a result of which they are correlated. $\mu_{pp'}$ is a sum of $2Q$ products of two correlated real Gaussian random variables. Invoking the CLT, $\mu_{pp'}$ can also be approximately normal with its mean and variance as

$$E[\mu_{pp'} | H_3] = Q\tilde{\sigma}_{p,1}\tilde{\sigma}_{p',2} \tag{9}$$

$$D[\mu_{pp'} | H_3] = \frac{Q}{2}\left[\zeta_{p,1}^2\zeta_{p',2}^2 + \tilde{\sigma}_{p,1}^2\tilde{\sigma}_{p',2}^2\right] \tag{10}$$

Then the CT can be simply designed as

$$\begin{cases} H_{012} : \mu_{pp'} \sim N\left(0, Q\zeta_{p,1}^2\zeta_{p',2}^2/2\right) \\ H_3 \ \ : \mu_{pp'} \sim N\left(Q\tilde{\sigma}_{p,1}\tilde{\sigma}_{p',2}, Q(\zeta_{p,1}^2\zeta_{p',2}^2 + \tilde{\sigma}_{p,1}^2\tilde{\sigma}_{p',2}^2)/2\right) \end{cases} \tag{11}$$

The optimal, in the Neyman-Pearson sense, detector is the likelihood ratio test (LRT), and it can be written as [12]

$$\lambda(\mu_{pp'}) = \frac{p(\mu_{pp'} | H_3)}{p(\mu_{pp'} | H_{012})} \underset{H_{012}}{\overset{H_3}{\gtrless}} \gamma \tag{12}$$

which can be simplified as,

$$l(\mu_{pp'}) = (\mu_{pp'} + D)^2 \underset{H_{012}}{\overset{H_3}{\gtrless}} \eta \tag{13}$$

with $D = Q\zeta_{p,1}^2\zeta_{p',2}^2 / \tilde{\sigma}_{p,1}\tilde{\sigma}_{p',2}$.

According to (13), the test statistic is chosen to be $l = (\mu_{pp'} + D)^2$, which has a noncentral chi-square distribution with one degree of freedom and noncentrality parameter D^2 under H_{012} and $(Q\tilde{\sigma}_{p,1}\tilde{\sigma}_{p',2} + D)^2$ under H_3. However, for a noncentral chi-square distribution with one degree of freedom, we can easily obtain its cumulative distribution function (CDF) based on that of a normal distribution,

$$F(l | H_{012}) = \frac{1}{2}\left[erf\left(\frac{\sqrt{l} - D}{\sqrt{Q\zeta_{p,1}^2\zeta_{p',2}^2}}\right) - erf\left(\frac{\sqrt{l} + D}{\sqrt{Q\zeta_{p,1}^2\zeta_{p',2}^2}}\right)\right] \tag{14}$$

$$\begin{aligned} F(l | H_3) = \frac{1}{2}\Bigg[& erf\left(\frac{\sqrt{l} - Q\tilde{\sigma}_{p,1}\tilde{\sigma}_{p',2} - D}{\sqrt{Q(\zeta_{p,1}^2\zeta_{p',2}^2 + \tilde{\sigma}_{p,1}^2\tilde{\sigma}_{p',2}^2)}}\right) \\ & - erf\left(\frac{\sqrt{l} + Q\tilde{\sigma}_{p,1}\tilde{\sigma}_{p',2} + D}{\sqrt{Q(\zeta_{p,1}^2\zeta_{p',2}^2 + \tilde{\sigma}_{p,1}^2\tilde{\sigma}_{p',2}^2)}}\right)\Bigg] \end{aligned} \tag{15}$$

where, $erf(\cdot)$ stands for the error function by $erf(x) \triangleq \int_0^x \frac{2}{\sqrt{\pi}} \exp(-z^2) dz$.

Due to the Neyman-Pearson criterion, with the constraint condition $P\{H_3 | H_{012}\} = P_l'$, the adaptive threshold η in (13) is given by

$$\eta = F^{-1}(1 - P_l' | H_{012}) \tag{16}$$

where P_l' is defined as the error probability under H_{012} in the CT.

Hence, $P\{H_{012} | H_3\}$ can be obtained as

$$P\{H_{012} | H_3\} = F(\eta | H_3) \tag{17}$$

Note that the average power of SCESs ($\zeta_{p,1}^2$, $\zeta_{p',2}^2$) and the jamming power ($\tilde{\sigma}_{p,1}^2$, $\tilde{\sigma}_{p',2}^2$) are all unknown. Here, their estimations are used as substitutions. Therein, the average power of SCESs ($\hat{\zeta}_{p,1}^2$, $\hat{\zeta}_{p',2}^2$) can be estimated using radar equations. The estimations of $\tilde{\sigma}_{p,1}^2$, $\tilde{\sigma}_{p',2}^2$ under H_3 are given by

$$\hat{\tilde{\sigma}}_{p,1}^2 = \hat{\zeta}_{p,1}^2 - \hat{\sigma}_{w,1}^2,\ \hat{\tilde{\sigma}}_{p',2}^2 = \hat{\zeta}_{p',2}^2 - \hat{\sigma}_{w,2}^2 \tag{18}$$

where $\hat{\sigma}_{w,1}^2$ and $\hat{\sigma}_{w,2}^2$ are the estimations of noise power in receiver 1 and 2 respectively, which are obtained in radar locking periods.

B. Proposed Discrimination Method

Based on the aforementioned correlation test, FTs can be identified by deciding that all the targets included in the combinations, which are tested to be H_3, are FTs.

Note that $(K+M)^2$ correlation tests are implemented in all, in which each target is tested with the number of $(K+M)$. Therefore, the rejection probability of PT, denoted by P_l, can be calculated as

$$\begin{aligned} P_l &\triangleq P\{\text{rejected as a FT} | \text{a PT}\} \\ &= P\{\text{at least one of } (K+M) \text{ CTs is rejected as } H_3\} \\ &= 1 - P\{l(\mu_{pp'}) \le \eta,\ \forall p' = 1, 2, ..., K+M\} \\ &= 1 - \left(1 - P_l'\right)^{(K+M)} \end{aligned} \tag{19}$$

Therefore, for a given P_l, P_l' in CTs should be set as

$$P_l' = 1 - (1 - P_l)^{1/(K+M)} \tag{20}$$

The proposed discrimination method can be derived as the following three steps.

- *Threshold decision*: For a given P_l, P_l' is calculated using (20) based on the number of detected targets.
- *Correlation test*: For every possible combinations consisting of two SCESs in receiver 1 and 2, CTs are implemented given in (11) and (13).
- *FTs discrimination*: Once a combination is tested to be H_3, two targets included in it are rejected as FTs, and the targets left are accepted as PTs.

C. Performance Analysis

To evaluate the performance of the proposed scheme, we introduce the acceptance probability of PT (P_{PT}) and the rejection probability of FT (P_{FT}).

- The **acceptance probability of PT** is defined as the probability of accepting a PT as PTs, and it can be obtained as

$$\begin{aligned} P_{PT} &\triangleq P\{\text{accepted as a PT} | \text{a PT}\} \\ &= 1 - P_l \end{aligned} \tag{21}$$

which is a constant for a previously given P_l.

- The **rejection probability of FT** is defined as the probability of rejecting a FT as FTs, i.e.,

$$\begin{aligned} P_{\text{FT}} &\triangleq P\{\text{rejected as a FT} | \text{a FT}\} \\ &= P\{\text{at least one of } (K+M) \text{ CTs is rejected as } H_3\} \\ &= 1 - P\{l(\mu_{pp'}) \le \eta,\ \forall p' = 1,2,...,K+M\} \\ &= 1 - P\{H_{012} | H_3\} \cdot P\{H_{012} | H_{012}\}^{K+M-1} \\ &= 1 - F(\eta | H_3) \cdot (1 - P_l')^{K+M-1} \end{aligned} \tag{22}$$

The exact expressions of P_{PT} (21) and P_{FT} (22) are obtained on the premise of *a priori* knowledge of jamming energy, echoes energy and noise energy in every receivers, which represents a benchmark to the performance of our discrimination method. Their estimation errors might inevitably lead to a deviation from (21) and (22). Furthermore, the normal approximation for the distribution of $\mu_{pp'}$ in (11) might also draw some deviations.

IV. Simulation Results

In this section, we consider multistatic radar consisting of a transmitter and two sufficiently spaced receivers, i.e., N = 2. Some simulation results are provided to demonstrate the performance of the proposed discrimination algorithm.

According to the fact that FTs are not implemented to jam the radar depending on the power, jamming-noise-ratio (JNR $= \tilde{\sigma}_{p,n}^2 / \sigma_{w,n}^2$) for FTs and signal-noise-ratio (SNR $= \sigma_{p,n}^2 / \sigma_{w,n}^2$) for PTs are assumed the same in both receivers and defined as target-noise-ratio (TNR).

A. Monte Carlo Simulations

Monte Carlo simulations are given first to verify the efficiency of the proposed approach. In order to simplify the simulation scenario, one PT is present in the detected area and two FTs are generated to resemble the PT, i.e., K = 1, M = 2.

In Fig. 1, the rejection probability of FT P_{FT} is given as a function of the number of PRIs Q where the threshold is set to ensure $P_l = 10^{-3}$. P_{FT} is obtained by both the obtained exact expression (22) and Monte Carlo simulations with 5000 trials. The curves in the figure correspond to different values of TNR, where TNR = 0, 3, 6, 9 dB.

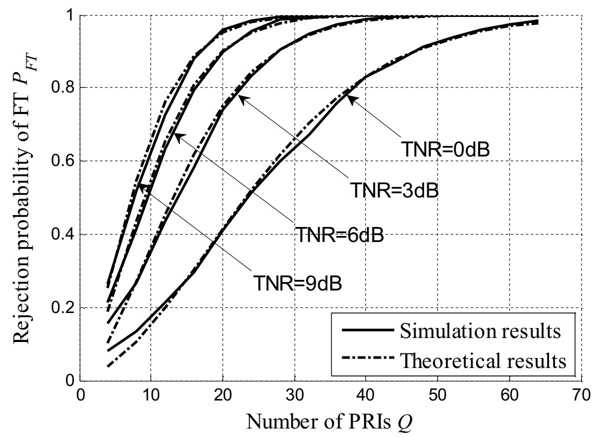

Fig. 1. Rejection probability of FT with $P_l = 10^{-3}$

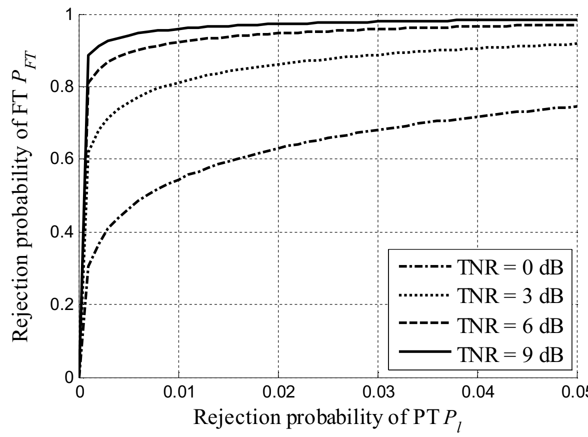

Fig. 2. Discrimination operating characteristic for different values of TNR (Q = 16, K = 1, M = 2)

Fig. 1 shows the feasibility of the discrimination method of FTs on the premise of the acceptance probability of PTs. And, the simulation results correspond to the theoretical results with little deviations caused by the aforementioned estimation errors and normal approximation. These deviations decrease with increasing value of Q. Moreover, it is evident that the discrimination performance becomes better with larger Q and higher TNR.

B. Discrimination Operating Characteristic (DOC)

Invoking the exact expression of P_{PT} (21), discrimination operating characteristic (DOC) is defined as the curve of P_{FT} as a function of P_l similar to the receiver operating characteristic (ROC), which can be used to evaluate the discrimination performance of the proposed approach.

Figs. 2-4 report the DOC for different values of TNR, the number of PRIs Q and the number of FTs M, respectively. In Fig. 2, one PT and two FTs are present in the scenario, and we set Q = 16, TNR = 0, 3, 6, 9 dB. In Fig. 3, there are still one PT and two FTs in the scenario, and TNR = 0 dB, Q = 16, 32, 48,

64. In Fig. 3, we have one PT in the scenario, and TNR = 3 dB, $Q = 16$, $M = 2, 4, 6, 8$.

From Figs. 2-4, some conclusions are obvious. We briefly summarize them as follows:

1. The larger P_l is given, the higher discrimination ratio of FT is obtained. All curves in these figures all pass through the origin (0,0), which represents that the threshold is set to positive infinity in order to get $P_l = 0$.

2. Higher TNR is, larger P_{FT} is for the same P_l, and better discrimination ability of FT is obtained.

3. The more PRIs are used; the higher discrimination ratio of FT is obtained.

4. The less FTs are present; the higher discrimination ratio of FT is obtained.

V. Conclusions

In this paper, a discrimination method of deception false targets by signal fusion has been proposed in multistatic radar system. Both theoretical analysis and simulations indicate the feasibility of the proposed approach. Furthermore, the merit of the method lies in that it can be used to identify FTs generated by deception signals with arbitrary modulation, because it just utilizes the difference in spatial scattering properties between PTs and FTs reflected by the mutual correlation of target echo signals.

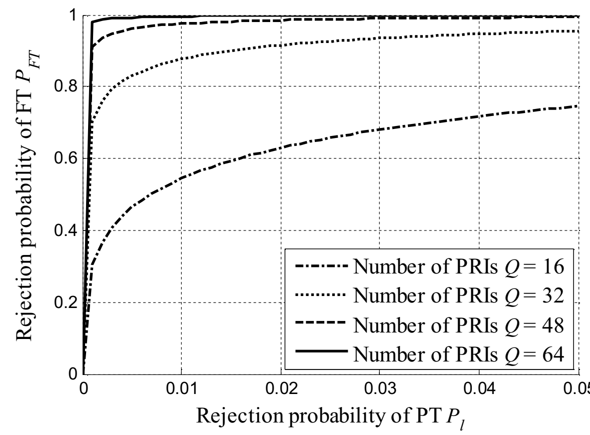

Fig. 3. Discrimination operating characteristic for different number of PRIs Q (TNR = 0 dB, $K = 1$, $M = 2$)

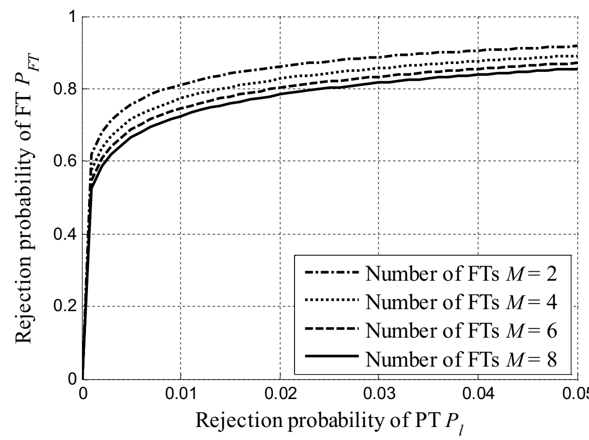

Fig. 4. Discrimination operating characteristic for different number of FTs M ($Q = 16$, TNR = 3 dB, $K = 1$)

References

[1] N.J. Li and Y.T. Zhang, "A survey of radar ECM and ECCM," IEEE Trans. on Aerospace and Electronic Systems, vol. 31, no. 3, pp. 1110-1120, July 1995.

[2] J. Akhtar, "Orthogonal block coded ECCM schemes against repeat radar jammers," IEEE Trans. on Aerospace and Electronic Systems, vol. 45, no. 3, pp. 1218-1226, July 2009.

[3] C. Huang, Z.M. Chen, and R. Duan, "Novel discrimination algorithm for deceptive jamming in polarimetric radar," Proc of the 2012 International Conference on Information Technology and Software Engineering, Berlin: Springer, pp. 369-365, 2013.

[4] B. Rao, S.P. Xiao, X.S. Wang, and T. Wang, "Maximum likelihood approach to the estimation and discrimination of exoatmospheric active phantom tracks using motion features," IEEE Trans. on Aerospace and Electronic Systems, vol. 48, no. 1, pp. 794-818, January 2012.

[5] M. Greco, F. Gini, and A. Farina, "Radar deception and classification of jamming signals belonging to a cone class," IEEE Trans. on Signal Processing, vol. 56, no. 5, pp. 1984-1993, May 2008.

[6] L. Yang and Z.K Sun, "Identification of false targets in bistatic radar system," Proc of the IEEE Aerospace and Electronics Conference, Dayton, pp. 878-883, July 1997.

[7] Y.L. Zhao, X.S. Wang, G.Y. Wang, Y.H. Liu, and J. Luo, "Tracking technique for radar network in the presence of multi-range-false-target deception jamming," Acta Electronica Sinica, vol. 35, no. 3, pp. 454-458, March 2007.

[8] B. Lv, Y. Song, and C.Y. Zhou, "Study of multistatic radar against velocity-deception jamming," Electronics, Communication and Control (ICEE), pp. 1044-1047, 2011.

[9] F.A. Butt, I.H. Naqvi, and A.I. Najam, "Radar ECCM against deception jamming: a novel approach using bi-static and mono-static radars," 15th International Multitopic Conference (INMIC), Islamabad, pp. 137-141, December. 2012.

[10] E. Fishler, A. Haimovich, R. Blum, D. Chizhik, L. Cimini, and R. Valenzuela, "MIMO radar: an idea whose time has come," Proc of the IEEE Radar Conference, Philadelphia, pp. 71-78, 2004.

[11] E. Fishler, A. Haimovich, R.S. Blum, L. Cimini, D. Chizhik, and R. Valenzuela, "Spatial diversity in radars-models and detection performance," IEEE Trans. on Signal Processing, vol. 54, no. 3, pp. 823-838, March 2006.

[12] H.L.V. Trees, Dectection a Estimated, and Modulation Theory, vol. 1, New York: Wiley, 1968.